Supplementary Figure 1

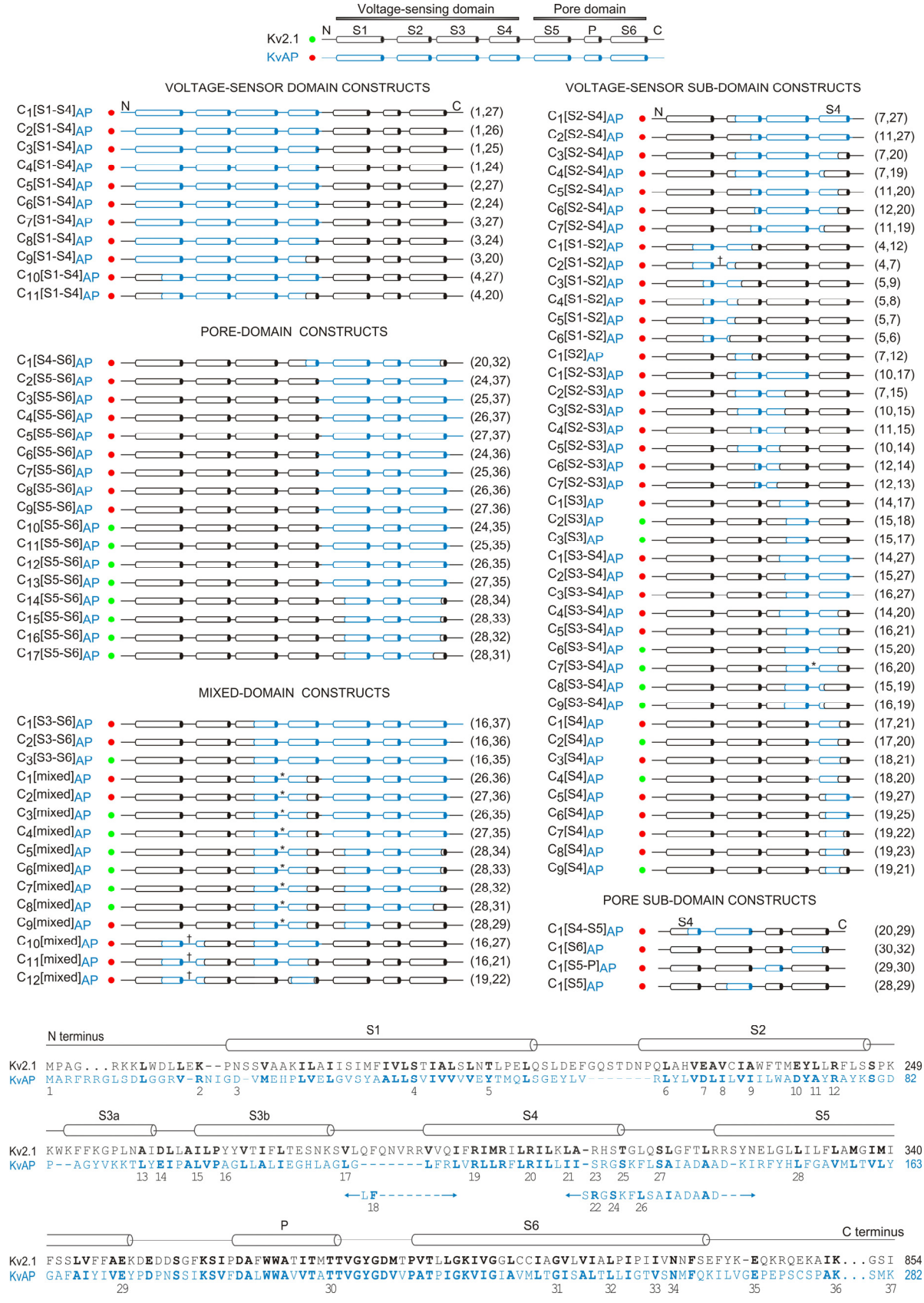

←

Supplementary Figure 1 Legend

Summary of chimeras constructed between KvAP and the Kv2.1 channel

Functional (green circles) and non-functional (red circles) constructs are named based on the region being transferred. Nomenclature on the left of each construct is Cx[region]donor channel where x is a chimera number assigned to constructs in each region starting from the largest (C1) to the smallest contiguous stretch of KvAP residues transferred in the region. Splice sites for each construct are coded to the right of the chimera and the code is depicted on the alignment of KvAP and Kv2.1 (below). Transferred regions include the labeled residue in KvAP. The splice sites indicated for C1-9[mixed]AP are for the regions added in the background of C7[S3-S4]AP (indicated with an asterisk). For C10-12[mixed]AP, splice sites are for the regions added in the background of C2[S1-S2]AP (indicated with a dagger). The two short KvAP sequences positioned below the full KvAP sequence indicate spice sites for several chimeras produced using shifted alignments.

Construct	$V_{1/2}$ (mV)	z
Kv2.1	-4.4 ± 0.9	2.7 ± 0.2
Shaker	-29 ± 2	3.2 ± 0.2
C6[S3-S4]AP	+9.5 ± 2.2	1.3 ± 0.1
C7[S3-S4] AP	+21 ± 2	1.2 ± 0.1
C*[S3-S4] AP	+47 ± 1	3.0 ± 0.1
C8[S3-S4] AP	+22 ± 1	1.1 ± 0.1
C9[S3-S4] AP	+14 ± 1	1.2 ± 0.1
C2[S3] AP	+25 ± 1	1.4 ± 0.1
C3[S3] AP	-57 ± 1[a]	2.6 ± 0.2
C2[S4] AP	-13 ± 1	2.2 ± 0.2
C4[S4] AP	+17 ± 1	1.4 ± 0.1
C9[S4] AP	-12 ± 1[a]	1.6 ± 0.1
C10[S5-S6] AP	> +100[b]	-
C11[S5-S6] AP	> +100[b]	-
C12[S5-S6] AP	> +100[b]	-
C13[S5-S6] AP	> +100[b]	-
C14[S5-S6] AP	< -50[c]	-
C15[S5-S6] AP	< -70[c]	-
C16[S5-S6] AP	> +80[b]	-
C17[S5-S6] AP	< 0[c]	-
C3[S3-S6] AP	> +100[b]	-
C3[mixed] AP	> +100[b]	-
C4[mixed] AP	> +100[b]	-
C5[mixed] AP	< +20[c]	-
C6[mixed] AP	< +20[c]	-
C7[mixed] AP	> +100[b]	-
C8[mixed] AP	< 0[c]	-

Supplementary Table 1

Gating properties of chimeras between KvAP (donor) and Kv2.1 or Shaker* (acceptor).

Voltage-activation relations were obtained from tail current measurements or by calculating conductance (G) from steady state current measurements and fitting with single Boltzmann functions to obtain approximate midpoint ($V_{1/2}$) and slope factors (z). Data for all constructs were obtained with n ≥ 3; mean values are ± S.E.M..

[a] This channel displays a second phase in the G-V relationship, and only the first phase was fit with a single Boltzmann function.

[b] This channel has a G-V relationship which does not saturate at voltages up to +130 mV.

[c] This channel contains a leak conductance at negative voltages up to -120 mV. As the holding voltage is shifted more negative, the midpoint of the G-V relationship also shifts to more negative voltages.

Mutant	$V_{1/2}$ (mV)	z
Shaker	-29 ± 2	3.2 ± 0.2
C*[S3-S4]AP	+47 ± 1	3.0 ± 0.1
P99A	> +100 [a]	-
A100V	+66 ± 2	2.5 ± 0.2
G101A	> +50 [a]	-
L102A	+54 ± 2	3.3 ± 0.2
L103A	+ 47 ± 2	2.9 ± 0.2
A104V	+69 ± 3	2.8 ± 0.2
L105A	+66 ± 2	2.8 ± 0.2
I106A	+78 ± 3	2.0 ± 0.2
E107A	+61 ± 2	2.0 ± 0.2
G108A	+47 ± 2	2.7 ± 0.2
H109A	+45 ± 2	4.0 ± 0.2
L110A	+72 ± 4	2.3 ± 0.2
A111V	+56 ± 2	2.6 ± 0.1
G112A	> +70 [a]	-
L113A	+58 [b]	1.0 ± 0.1
G114A	+72 ± 1	2.5 ± 0.2
L115A	+102 ± 2	2.3 ± 0.2
F116A	-12 ± 2	2.5 ± 0.2
R117A	+54 ± 3	4.8 ± 0.2
L118A	+60 ± 2	3.0 ± 0.2
V119A	-22 ± 1	3.2 ± 0.1
R120A	+114 ± 3 [b]	1.3 ± 0.1
L121A	+6.7 ± 1.3	2.6 ± 0.2
L122A	> +60 [a,c]	-
R123A	+99 ± 2	1.5 ± 0.1
I124A	+2.6 ± 1.5	3.4 ± 0.2
L125A	+67 ± 2	2.6 ± 0.2
R126A	-24 ± 2	2.1 ± 0.2
I127A	> +70 [a]	-

Supplementary Table 2

Gating properties of C*[S3-S4]AP mutants.

Voltage-activation relations were obtained from tail current measurements or by calculating conductance (G) from steady state current measurements and fitting with single Boltzmann functions to obtain approximate midpoint ($V_{1/2}$) and slope factors (z). Numbering of point mutations in C*[S3-S4]AP corresponds to the sequence of KvAP. Data for all constructs were obtained with $n \geq 3$; mean values are $\pm$ S.E.M..

[a] These channels have G-V relationships which do not saturate at voltages up to +100 mV.

[b] These channels have very slow activation kinetics, with time courses that do not reach steady-state even with 1 sec test depolarizations.

[c] This channel contains a leak conductance at voltages negative of -40 mV.

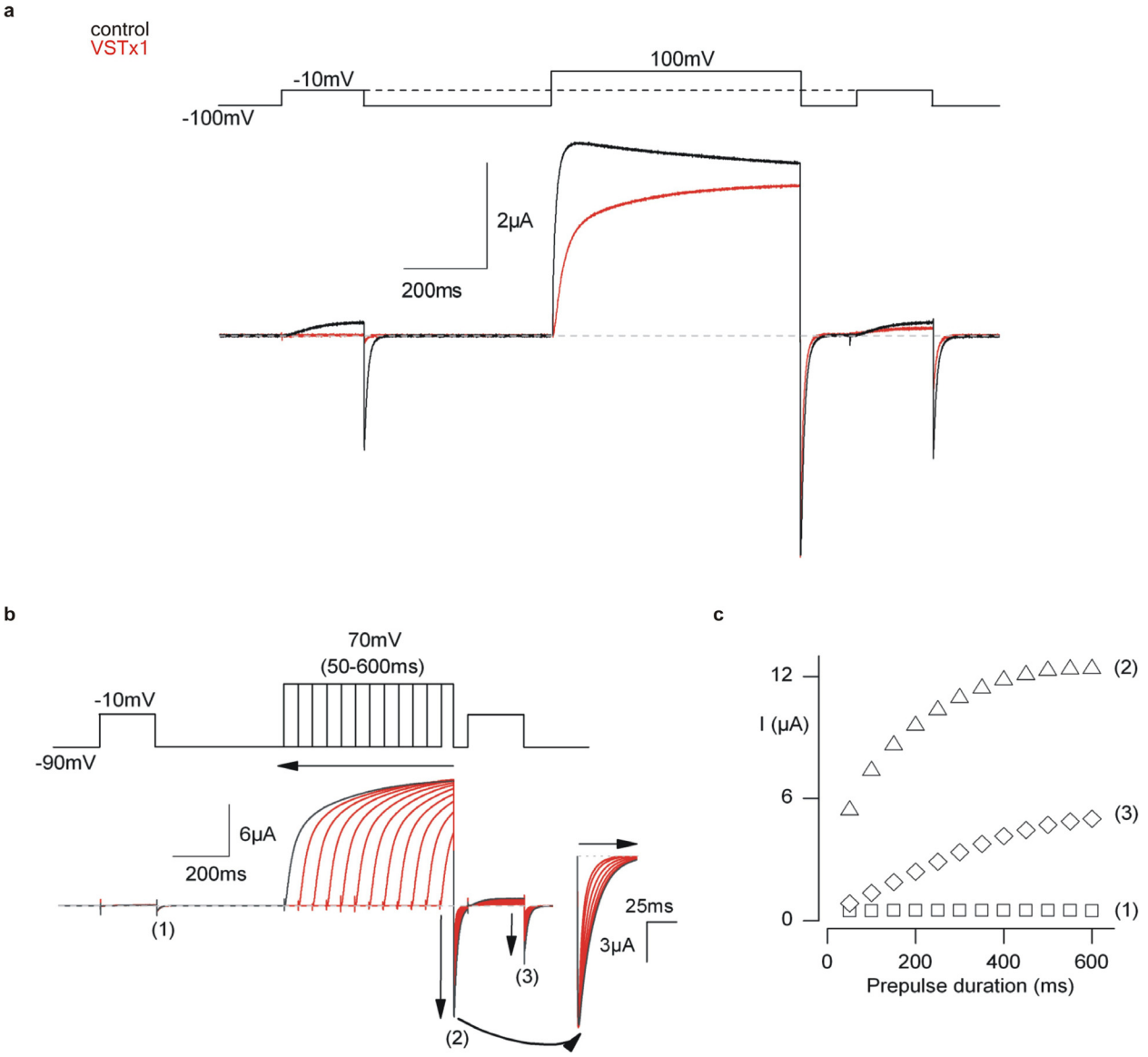

Supplementary Figure 2

Gating of Kv channels in the presence of VSTx1 and toxin dissociation from activated channels

Results: To examine whether VSTx1 unbinds from the C2[S4]AP chimera during strong depolarizations, we used a voltage protocol (Supplemental Fig 2a) consisting of a strong depolarization to +100 mV that is flanked by weak depolarizing steps to -10 mV, which should report on toxin occupancy of the channel because -10 mV is too weak to open toxin-bound channels (see Fig 2c in main paper). Following 600 ms strong depolarizations we see a significant change in the extent of inhibition at -10 mV (Supplemental Fig 2a), pointing to a change in toxin occupancy of the channel. Inspection of the kinetics of channel deactivation (closing) upon repolarization from +70 mV to -90 mV supports the notion that depolarization promotes toxin dissociation, but also suggests that toxin bound channels can open before the toxin unbinds. When strong depolarizations are applied for only 50 ms, channel deactivation is faster than control channels in the absence of toxin, but when they are applied for 600 ms, channel deactivation slows to near that observed in control (Supplemental Fig 2b and insert).

Legend: a, Relief of toxin inhibition by a 700 ms prepulse to 100 mV. VSTx1 concentration is 10 μM. **b,** Relationship between prepulse duration and relief of toxin inhibition. Inset shows scaled tail currents for (in ms) 50, 100, 200, 300, 400, 500 and 600 prepulse durations. Arrows indicate the direction of increasing prepulse duration, prepulse tail current amplitude (2), relief of toxin inhibition (3), and decreasing deactivation kinetics (in inset). Dark gray color denotes the trace with the longest prepulse. **c,** Plot of tail current amplitudes for pulses (1), (2) and (3) as a function of prepulse duration.

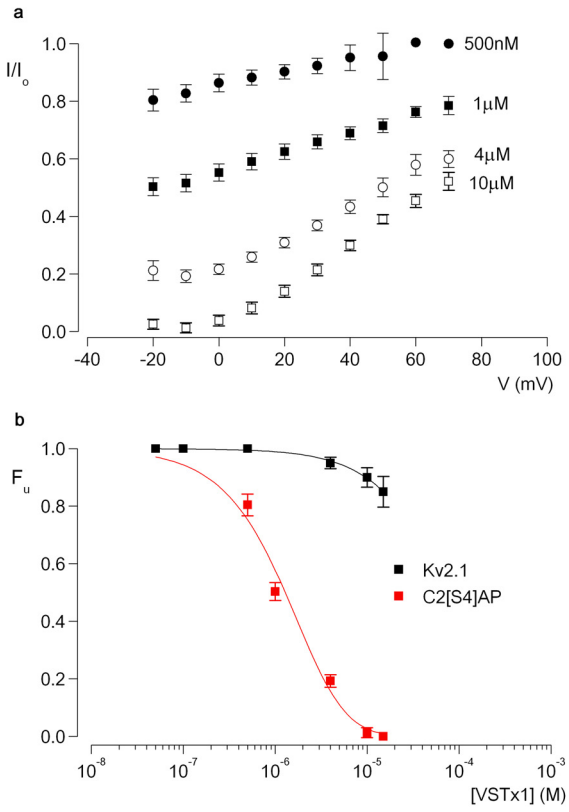

Supplementary Figure 3

Concentration-dependence for inhibition by VSTx1.

a, Voltage-dependent inhibition of chimera C2[S4]AP by VSTx1. Fraction of uninhibited tail currents (I/I_o) elicited by various strength depolarizations in the presence of varying concentrations of VSTx1. **b,** F_u measured at negative voltages (-20 mV) plotted as a function of VSTx1 concentration for Kv2.1 (black, K_d = 360 ± 9 μM) and C2[S4]AP (red, K_d = 6.2 ± 0.6 μM). Solid lines are a fit of $F_u = ([VSTx1]/([VSTx1] + K_d))^4$ to each data set, assuming four independent toxin binding sites per channel. n = 3-7 for each toxin concentration and error bars ± S.E.M..

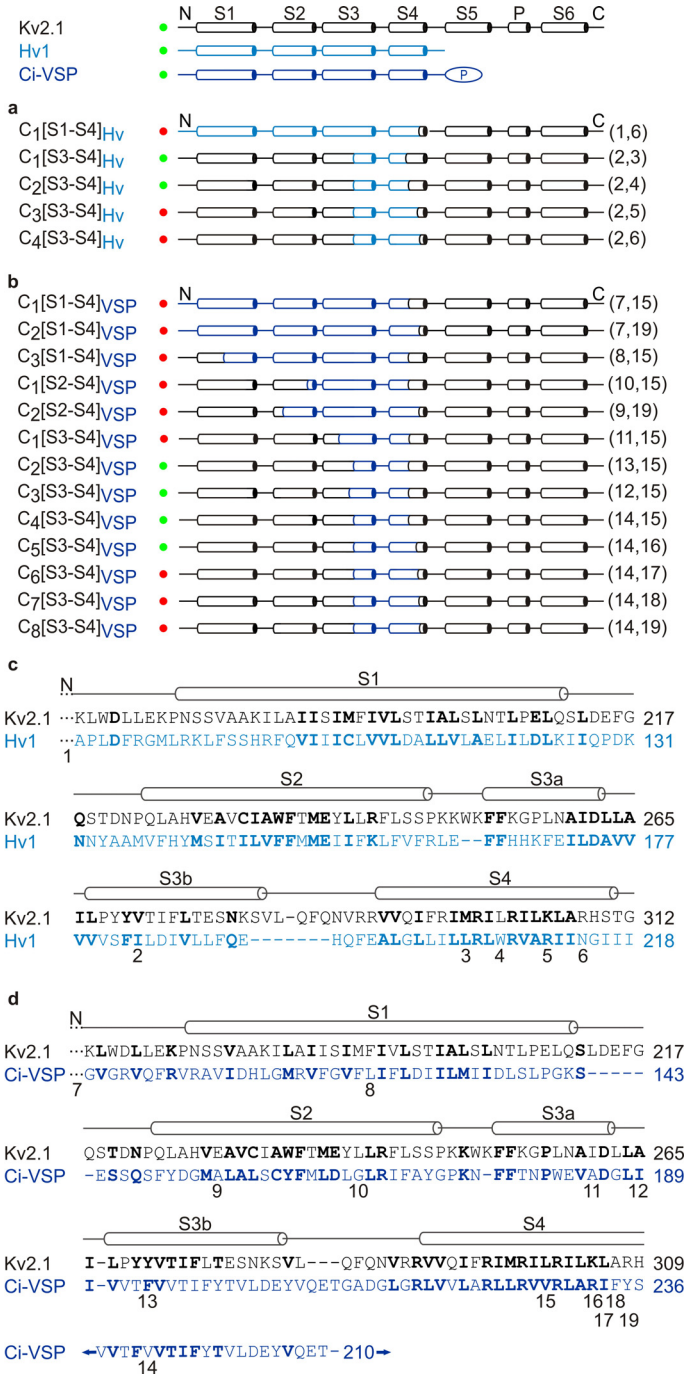

Supplementary Figure 4

Summary of chimeras constructed between voltage-sensing proteins and the Kv2.1 channel

a, b Depiction of chimeras between Hv1 or Ci-VSP and Kv2.1. Functional (green circles) and non-functional (red circles) constructs are named based on the region being transferred. Nomenclature on the left of each construct is Cx[region transferred]donor channel, where x is a chimera number assigned to constructs in each region. Splice sites for each construct are coded to the right of the chimera and the code is depicted on the alignment in c and d. **c,** Alignment of Hv1 and Kv2.1 indicating splice sites used for generating the chimeras in a. Transferred regions include the labeled residue in Hv1. **d,** Alignment of Ci-VSP and Kv2.1 indicating splice sites used for generating the chimeras in b. Transferred regions include the labeled residue in Ci-VSP. Chimeras involving splice site 14 were constructed with a shifted alignment, as shown.

Construct	$V_{1/2}$ (mV)	z
C1[S3-S4]Hv	-31.6 ± 1.5 [a]	1.6 ± 1.2
C2[S3-S4]Hv	-15.8 ± 0.5	2.1 ± 0.4
C2[S3-S4]VSP	-7.9 ± 1.6[a]	1.8 ± 1.2
C3[S3-S4]VSP	39.9 ± 0.8	1.6 ± 0.5
C4[S3-S4]VSP	-[b]	-
C5[S3-S4]VSP	-[c]	-

Supplementary Table 3

Gating properties of chimeras between voltage-sensing proteins and Kv2.1 channels

Tail current-voltage activation relations were fit with a single Boltzmann function to obtain approximate midpoint ($V_{1/2}$) and slope factors (z).
Data for all constructs were obtained with n ≥ 3; mean values are ± S.E.M..
[a] The channel displays a second phase in the G-V relationship, and only the first phase was fit with a single Boltzmann function.
[b] The channel begins to activate at voltages positive to -80 mV, but the G-V does not reach a maximum even at voltages as positive as +40 mV.
[c] This chimera begins to activate at voltages positive to +60 mV, but the G-V does not reach a maximum at the most positive voltages (+120 mV) examined.

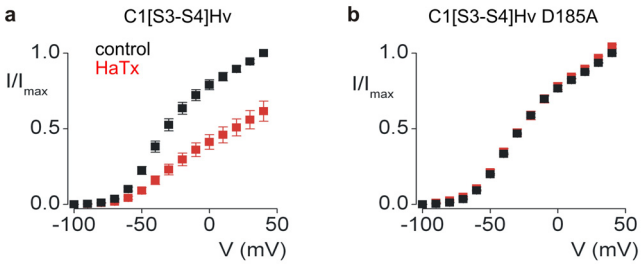

Supplementary Figure 5

The D185A mutant renders the Hv1 paddle chimera insensitive to HaTx.

a, Tail current voltage-activation relations for the C1[S3-S4]Hv chimera in control (black) and the presence of 2 μM HaTx (red) obtained after expression of the chimera in oocytes. Test depolarizations were 300 ms in duration, and both holding and tail voltages were -90 mV. **b,** Tail current voltage-activation relations for the D185A mutant of C1[S3-S4]Hv as in a. D185 is the only Asp within the transferred region and is positioned near the N-terminal end of the region transferred from Hv1 into Kv2.1 (see Fig 4 in main text). Numbering corresponds to the full Hv1 sequence. For all voltage-activation relations n = 3 and error bars ± S.E.M..

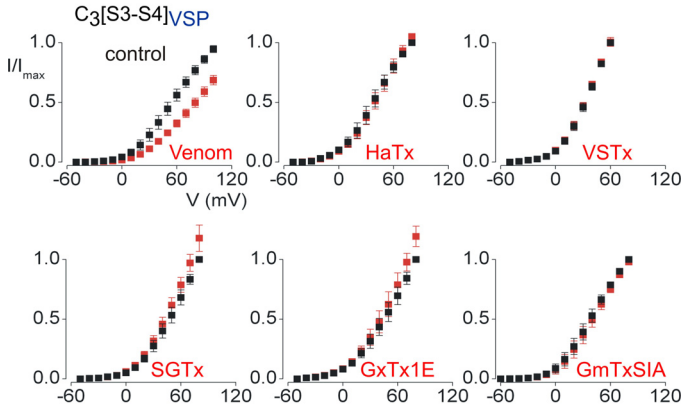

Supplementary Figure 6

Sensitivity of a Ci-VSP paddle chimera to tarantula toxins.

Voltage-activation relations in the absence (black) and presence (red) of tarantula venom/toxins for a chimera containing the paddle of Ci-VSP in the Kv2.1 channel after expression in oocytes. Potassium currents were recorded using 400-700 ms test depolarizations from holding voltages between -100 and -80 mV, and a tail voltage of -50 mV. Venom was applied at a 1:2000 dilution and toxin concentrations (in μM) were 1.5 for HaTx, 8 for VSTx1, 4 for SGTx1, 1 for GxTx1E and 5 for GmTxSIA. For all voltage-activation relations n = 3-4 and error bars ± S.E.M..